Inversion of Magnetic Data from Remanent and Induced Sources

Robert G. Ellis
Geosoft Inc.
Suite 810, 207 Queens Quay West,
Toronto, ON, Canada
Robert.Ellis@Geosoft.com

Barry de Wet
Ivanhoe Australia Ltd.
Level 13, 484 St Kilda Road
Melbourne, VIC, 3004, Australia
BarryW@Ivancorp.net

Ian N. Macleod
Geosoft Inc.
Suite 810, 207 Queens Quay West,
Toronto, ON, Canada
Ian.Macleod@Geosoft.com

SUMMARY

Magnetic field data are of fundamental importance in many areas of geophysical exploration with 3D voxel inversion being a common aid to their interpretation. In the majority of voxel based inversions it is assumed that the magnetic response arises entirely from magnetic induction. However, in the last decade, several studies have found that remanent magnetization is far more prevalent than previously thought. Our experience with numerous minerals exploration projects confirms that the presence of non-induced magnetization is the rule rather than the exception in base metals exploration.

In this work we show that failure to accommodate for remanent magnetization in 3D voxel-based inversion can lead to misleading interpretations. We present a technique we call Magnetization Vector Inversion (MVI), which incorporates both remanent and induced magnetization without prior knowledge of the direction or strength of remanent magnetization. We demonstrate our inversion using model studies and field data. Successful application to numerous minerals exploration surveys confirms that incorporating remanent magnetization is essential for the correct interpretation of magnetic field data.

Key words: inversion, 3D, remanent magnetization, magnetization vector inversion.

INTRODUCTION

The utility of magnetic field data in many areas of geophysical exploration is well-known as is the application of 3D voxel inversion to aid in magnetic data interpretation (for example, Li and Oldenburg 1996, Pilkington, M., 1997, Silva et al. 2000, Zhdanov and Portniaguine 2002, to cite just a few). In the majority of voxel based inversions it is assumed that the magnetic response arises entirely from magnetic induction. However, in the last decade, studies have found that remanent magnetization is far more prevalent than previously thought (McEnroe et al. 2009) and affects crustal rocks as well as zones of mineralization. Unfortunately, remanent magnetization can seriously distort inversion based on the assumption that the source is only induced magnetization. The severity of the distortion is due to the highly non-unique nature of potential field inversion making it extraordinarily easy for a potential field inversion to produce a seemingly plausible model which agrees satisfactorily with the observed data, even when a fundamental assumption in the inversion is flawed.

Several authors have reported progress toward magnetic data inversions including remanent effects (for example, Shearer and Li 2004, Kubota and Uchiyama 2005, Lelièvre and Oldenburg 2009). In this work we report further progress in this direction with a technique we call Magnetization Vector Inversion (MVI), which incorporates both remanent and induced magnetization without prior knowledge of the direction or strength of remanent magnetization. In the following sections, we extend conventional scalar susceptibility inversion to a magnetization vector inversion, that is, we allow the inversion to solve for the source magnetization amplitude and direction. While this increases the number of variables in the inversion we will show by example that the same regularization principles that allow compact targets to be resolved in highly unconstrained scalar susceptibility inversion also apply in vector inversion.

Perhaps our most significant finding is that MVI, or more generally, inversion including all forms of magnetization, significantly improves the interpretation of the majority of minerals based magnetic field inversions. Unfortunately, the surprising degree of improvement in interpretability cannot be adequately presented in a paper and can only be verified by direct experience. Consequently, while we have applied MVI to a large number of magnetic field surveys and find the results to be significantly superior to conventional scalar based inversion, in this paper we are forced to limit our attention to a synthetic case and field data from the Cu-Au Osborne deposit located approximately 195km SE of Mount Isa, in Western Queensland, Australia.

METHOD AND RESULTS

Let us begin with the very general assumption that the magnetic properties of the earth can be represented by a volume magnetization, $\boldsymbol{M}(\boldsymbol{r})$ (Telford et al. 1990). We make no assumptions about whether source of the magnetization is induced, remanent, or otherwise.

From magnetostatics, the magnetic field $\boldsymbol{B}$ at point $\boldsymbol{r_j}$ resulting from a volume V containing magnetization, $\boldsymbol{M}(\boldsymbol{r})$, is given by

$$\boldsymbol{B}(\boldsymbol{r_j}) = \nabla \int_V \boldsymbol{M}(\boldsymbol{r}) \cdot \nabla \frac{1}{|\boldsymbol{r} - \boldsymbol{r_j}|} dr^3 \qquad (1)$$

This expression shows directly that the magnetization vector $\mathrm{M}(\mathrm{r})$ is the natural parameter for inversion. This is a crucial observation.

If the volume V consists of a collection of N sub-volumes v_k each of constant magnetization m_k then

$$B_\beta(\boldsymbol{r_j}) = \sum_{k,\alpha}^{N,3} m_{k,\alpha} \int_{v_k} \partial_\alpha \partial_\beta \frac{1}{|\boldsymbol{r} - \boldsymbol{r_j}|} dr^3 \qquad (2)$$

This defines the forward problem: given a set of sources $\boldsymbol{m}_k$ $(k = 1,..,N)$ then $\boldsymbol{B_j}$ is the predicted magnetic field anomaly at points, $\boldsymbol{r}_j$ $(j = 1,..,M)$. Note that the coordinate index α is summed over indicating that we are free to choose the most computationally convenient internal coordinate system. It also suggests that a coordinate invariant quantity, such as the amplitude, $M(r) = |\boldsymbol{M}(\boldsymbol{r})|$, will be most robustly determined from the data.

For conciseness, we will represent Eq (2) simply as

$$\boldsymbol{B} = \boldsymbol{G}\,\boldsymbol{m} \qquad (3)$$

The vector magnetization inverse problem is defined as solving for $\boldsymbol{m}$ given $\boldsymbol{B}$ subject to an appropriate regularization condition. Although there are many choices for the regularization (see for example, Zhdanov 2002), we choose without loss of generality, the familiar Tikohonov minimum gradient regularizer. The inverse problem becomes solving for $\boldsymbol{m}$ in,

$$\begin{aligned} &\text{Min } \phi(\boldsymbol{m}) = \phi_D(\boldsymbol{m}) + \lambda\,\phi_M(\boldsymbol{m}) \\ &\phi_D(\boldsymbol{m}) = \sum_j^M \left| \frac{\boldsymbol{G_j}\,\boldsymbol{m} - \boldsymbol{B_j}}{e_j} \right|^2 \qquad (4) \\ &\phi_M(\boldsymbol{m}) = \sum_\gamma^3 \left| w_\gamma \partial_\gamma \boldsymbol{m} \right|^2 + |w_0 \boldsymbol{m}|^2 \\ &\lambda : \ \phi_D(\boldsymbol{m}) = \chi_T^2 \end{aligned}$$

where in the first line, the total objective function ϕ is the sum of a data term ϕ_D and a model term ϕ_M with a Tikohonov regularization parameter, λ. The second line defines the data objective function in terms of the data equation (3) and the error associated with each data point, e_j. The third line gives the model objective function in terms of the gradient of the model $\partial_\gamma \boldsymbol{m}$ and the amplitude of the model, with weighting terms as required, w_γ, w_0. The fourth line indicates that the Tikohonv regularization parameter λ is chosen based on a satisfactory fit to the data in a chi-squared sense, χ_T^2. In addition, other constraints, such as upper and lower bounds, can be placed on $\boldsymbol{m}$ as appropriate to the specific exploration problem.

Example - Buried Prism

Although the buried prism model is far too simplistic to have exploration significance, it does make an excellent pedagogical example, so we follow tradition and begin by considering the inversion of simulated TMI data over a buried prism with magnetization vector $\boldsymbol{M}$ perpendicular to the earth field. The model consists a cube with side length 40m buried with a depth to top of 20m and a magnetization vector in the EW direction, $(M_y = 0,\ M_z = 0)$ as shown in Figure 1.

Simulated TMI data are shown in Figure 2 for Earth field with inclination 90° and amplitude 24000 nT. Cardinal directions have been chosen only for simplicity of explanation; any directions could be chosen with equivalent results. Also for simplicity, the data were simulated at 20m constant clearance and on a regular 8m grid.

Inverting the TMI data in Figure 2 yields the model shown in Figure 3 which should be compared to the true model shown in Figure 1. There is some variability in the magnetization direction but the predominant direction is clearly EW, in agreement with the true model.

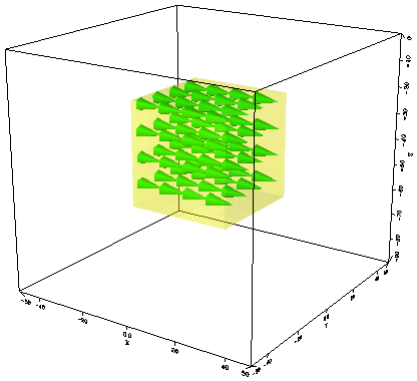

Figure 1: The buried prism model with magnetization vector orientation (Easterly) shown by the green cones. Side=100m

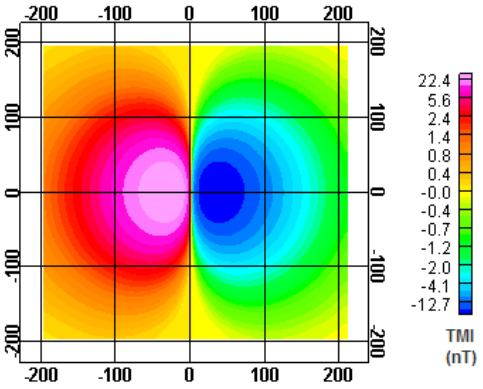

Figure 2: The TMI data simulated over the magnetization vector model shown in Figure 1. The axes are in metres.

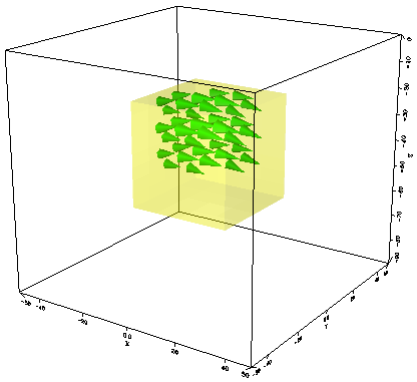

Figure 3: The MVI recovered model for comparison with Figure 1. The magnetization vector orientation shown by the green cones.

Vector magnetization models in 3D are difficult to interpret directly in all the but the simplest cases. In real-world exploration we need some simpler derived scalars which highlight the important information in the vector model. As suggested by Eq(1), the most robust and meaningful scalar is the amplitude of the vector magnetization and this should be

the primary quantity used in interpretation. However, since the magnetization vector direction is the earth field direction for induced sources, it is tempting to attempt to use the directional information recovered in MVI to generate scalars related to the earth field direction.

There are many possibilities but we have found that three useful derived scalars for exploration are: the amplitude of the magnetization, the earth field projection of the magnetization, and the amplitude of the perpendicular-to-earth-field components of the magnetization. In exploration problems, the amplitude is robust by being independent on of any assumptions regarding the earth field, while the amplitude perpendicular is an approximate indicator of non-induced magnetization. To support our findings, these three derived scalars are shown in Figure 4b, c, d for an East-West slice through the model volume bisecting the target in the true model.

In exploration situations it is convenient to present MVI output $\boldsymbol{M}$ normalized by the amplitude of the earth's magnetic intensity in the area of interest. That is, our results are displayed as $\boldsymbol{M}/H_E$ where H_E is the amplitude of the earth's magnetic intensity in the area of interest. By using this normalization in an area of purely induced magnetization, the numerical values returned by MVI inversion will be directly comparable to those of scalar susceptibility inversion, in our case in SI.

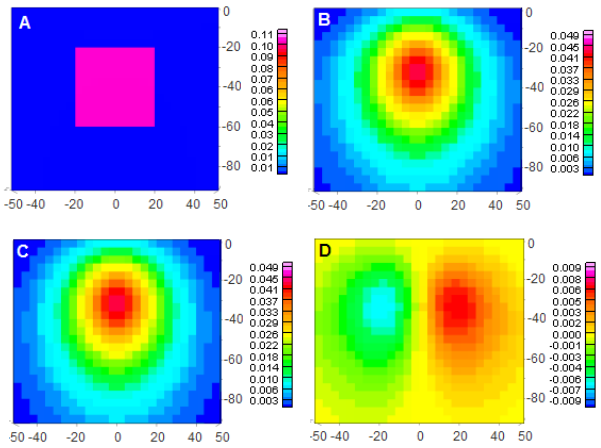

Figure 4: (a) A cross section through the true model, (b) the recovered amplitude of the magnetization vector, (c) the amplitude of the perpendicular-to-earth-field components of the magnetization, (d) the projection of the magnetization on to the earth field direction. The colour scales indicate the MVI magnetization in normalized to SI (see text).

For completeness, and to show the contrast between MVI and conventional scalar inversion, Figure 5b shows the equivalent section through a model produced by an inversion which assumes only induced magnetization. As should be expected, the recovered model using scalar inversion is a *very* poor representation of the true model, which in real-world exploration ultimately adds significant confusion to the interpretation process.

This simple prism example demonstrates the power of magnetization vector inversion and its advantage over scalar susceptibility inversion in cases where the magnetization vector direction deviates from the earth field direction. We argue that this situation predominates in real-world exploration environments based on experience from many magnetic surveys, however this cannot be shown here.

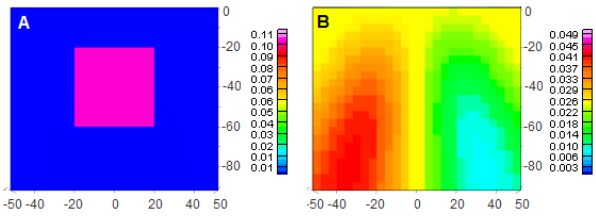

Figure 5: (a) A cross section through the true model, (b) the recovered scalar susceptibilty. The color bar shows the susceptibility magnitude in SI.

Example - Osborne

The preceding pedagogical study of MVI on simulated data over a prism provides a solid basis for the much more important application of MVI to field data. As mentioned in the Introduction, it is hard to appreciate fully the impact on magnetic data interpretation by including non-induced magnetic sources. However, to motivate our assertion, we present typical results taken from TMI data collected over the Osborne deposit.

The history of the Osborne mine is well described elsewhere, see for example, Rutherford et al. 2005. Briefly, significant Cu-Au mineralization beneath 30-50m of deeply weathered cover was confirmed in 1989. Intense drilling between 1990 and 1993 defined a total measured and indicated resource of 11.2 Mt at 3.51% Cu and 1.49 g/t Au. Exploration since 1995 has delineated high-grade primary mineralization dipping steeply East to some 1100 m vertical depth. As of 2001, total mined, un-mined and indicated resources are reported to be about 36 Mt and 1.1%Cu and 1 g/t Au (Tullemans et al. 2001). Current exploration is focussed on mapping the high-grade mineralization to greater depths and mapping similar structures in the surrounding area. The geophysics includes total magnetic intensity (TMI) data over the property, which is shown in Figure 6. The TMI data were acquired in 1997 flown at 40m clearance on 40m line spacing.

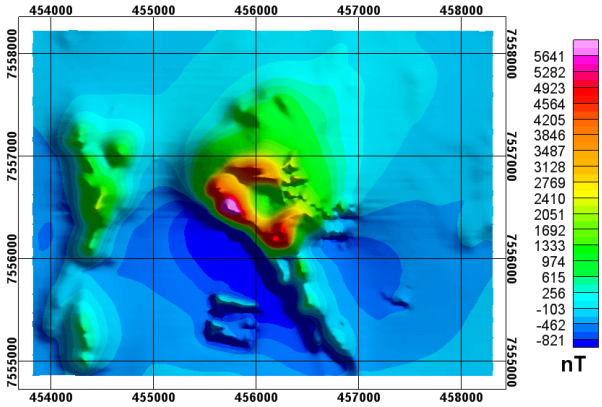

Figure 6: The observed TMI data acquired over the Osborne property. The axes are in metres. The color scale shows the TMI amplitude in nT.

Magnetization Vector Inversion of the Osborne TMI data yields the magnetization vector amplitude earth model shown in Figure 7. Superimposed (in black) is the subsequently discovered mineralization from extensive drilling and underground mining. For comparison, Figure 8 shows the corresponding scalar susceptibility inversion. Comparing

Figure 7 and Figure 8 shows that inverting for the magnetization vector provides a much better model for interpretation. The scalar inversion fails to represent reality in this case suggesting, most likely, that the scalar assumption is violated: a common occurrence in mineral exploration in our experience. In contrast the MVI model is consistent with the drilling results, and furthermore, indicates a steeply dipping volume on the Eastern flank. The strong near surface anomaly to the west of the dipping zone is known banded ironstone.

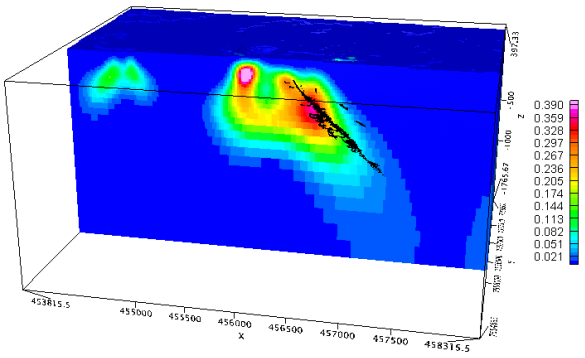

Figure 7: An EW section through the recovered MVI model amplitude at the Osborne property with the now known mineralization shown in black. The color bar gives the normalized amplitude in SI. The axes are in metres.

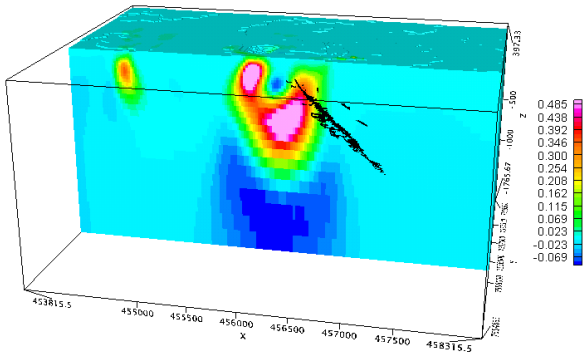

Figure 8: The same section as in Figure 7 for the scalar model with drilling and mineralization in black. The color bar gives the susceptibility in SI. The axes are in metres.

CONCLUSIONS

We have argued that remanent magnetization must be included in magnetic field data inversion in order to avoid seriously misleading interpretations. To support this argument we demonstrated the value of Magnetization Vector Inversion using model studies, and field data from the Osborne property. The degree of improvement afforded by using MVI in all areas of magnetic field data inversion may seem surprising, however recent advances in understanding remanent magnetism suggest that non-induced magnetization plays a far more important role than previously thought in the origin of magnetic anomalies. Successful application to numerous minerals exploration surveys confirms that incorporating remanent magnetization is recommended for the correct interpretation of the majority of magnetic field data.

ACKNOWLEDGMENTS

The authors would wish to thank Geosoft Inc. and Ivanhoe Australia Ltd. for permission to publish this work.

REFERENCES

Butler, R. F., 1992, Paleomagnetism: magnetic domains to geologic terranes, Blackwell Scientific Publications.

Kubota, R., and Uchiyama A., 2005, Three-dimensional magnetization vector inversion of a seamount, Earth Planets Space, 57, 691–699

Li, Y., and D. W. Oldenburg, 3-D inversion of magnetic data, Geophysics, 61, 1996, 394-408.

Lelièvre, P. G., and Oldenburg, D. W., 2009, A 3D total magnetization inversion applicable when significant, complicated remanence is present, Geophysics, 74, L21-L30

McEnroe, S. A., Fabian, K., Robinson, P., Gaina, C., Brown, L., 2009, Crustal Magnetism, Lamellar Magnetism and Rocks that Remember, Elements, 5, 241-246.

Pilkington, M., 1997, 3-D magnetic imaging using conjugate gradients, Geophysics, 62, 1132-1142.

Rutherford, N. F., Lawrance, L. M., and Sparks, G., 2005, Osborne Cu-Au Deposit, Clonclurry, North West Queensland, CRC LEME Report.

Shearer, S., and Y. Li, 2004, 3D Inversion of magnetic total gradient data in the presence of remanent magnetization: 74th Annual Meeting, SEG, Technical Program, Expanded Abstracts, 23, 774-777.

Silva, J. B. C., Medeiros, W. E., and Barbosa, V. C. F., 2001, Potential-field inversion: Choosing the appropriate technique to solve a geologic problem, Geophysics, 66, 511 - 520.

Telford, W. M., Geldart, L. P., Sherriff, R. E., and Keys, D. A., 1990, Applied Geophysics, Cambridge University Press.

Tullemans, F. J., Agnew P., and Voulgaris, P., 2001, The Role of Geology and Exploration Within the Mining Cycle at the Osborne Mine, NW Queensland, in Monograph 23 - Mineral Resource and Ore Reserve Estimation - The AusIMM Guide to Good Practice, Australian Institute of Mining and Metallurgy, Melbourne, 157-168.

Zdhanov, M. S., 2002, Geophysical Inverse Theory and Regularization Problems, Method in Geochemistry and Geophysics 36, Elsevier Science B.V., Amsterdam, The Netherlands.

Zhdanov, M. S., and Portniaguine, O., 2002, 3-D magnetic inversion with data compression and image focusing, *Geophysics*, 67, 1532-1541